Published online 4 March 2011

Nucleic Acids Research, 2011, Vol. 39, No. 12 ***5003–5014***
doi:10.1093/nar/gkr119

Massive production of small RNAs from a non-coding region of *Cauliflower mosaic virus* in plant defense and viral counter-defense

Todd Blevins[1,2], Rajendran Rajeswaran[1], Michael Aregger[1], Basanta K. Borah[1], Mikhail Schepetilnikov[1], Loïc Baerlocher[3], Laurent Farinelli[3], Frederick Meins Jr[2], Thomas Hohn[1] and Mikhail M. Pooggin[1,*]

[1]Institute of Botany, University of Basel, Schönbeinstrasse 6, 4056 Basel, [2]Friedrich Miescher Institute for Biomedical Research, Maulbeerstrasse 66, 4058 Basel and [3]Fasteris SA, Ch. du Pont-du-Centenaire 109, 1228 Plan-les-Ouates, Switzerland

Received December 21, 2010; Revised February 14, 2011; Accepted February 15, 2011

ABSTRACT

To successfully infect plants, viruses must counteract small RNA-based host defense responses. During infection of *Arabidopsis,* Cauliflower mosaic pararetrovirus (CaMV) is transcribed into pregenomic 35S and subgenomic 19S RNAs. The 35S RNA is both reverse transcribed and also used as an mRNA with highly structured 600 nt leader. We found that this leader region is transcribed into long sense- and antisense-RNAs and spawns a massive quantity of 21, 22 and 24 nt viral small RNAs (vsRNAs), comparable to the entire complement of host-encoded small-interfering RNAs and microRNAs. Leader-derived vsRNAs were detected bound to the Argonaute 1 (AGO1) effector protein, unlike vsRNAs from other viral regions. Only negligible amounts of leader-derived vsRNAs were bound to AGO4. Genetic evidence showed that all four Dicer-like (DCL) proteins mediate vsRNA biogenesis, whereas the RNA polymerases Pol IV, Pol V, RDR1, RDR2 and RDR6 are not required for this process. Surprisingly, CaMV titers were not increased in *dcl1/2/3/4* quadruple mutants that accumulate only residual amounts of vsRNAs. Ectopic expression of CaMV leader vsRNAs from an attenuated geminivirus led to increased accumulation of this chimeric virus. Thus, massive production of leader-derived vsRNAs does not restrict viral replication but may serve as a decoy diverting the silencing machinery from viral promoter and coding regions.

INTRODUCTION

Multicellular eukaryotes have evolved conserved, small RNA (sRNA)-generating pathways that regulate gene expression and silence transposons (1,2). In plants and some animals, sRNA pathways also have crucial functions in antiviral defense (3,4). Viral small RNA (vsRNA) duplexes processed from longer double-stranded RNAs (dsRNA) feed a cycle of viral RNA degradation, which spawns silencing signals that hinder viral spread (4). As a counter-defense, viruses express silencing-suppressor proteins able to block RNA silencing mechanisms of the host. Demonstrated activities of these suppressors include dsRNA binding to block vsRNA biogenesis, sequestration of vsRNA duplexes and inhibition of Argonaute protein (AGO)-mediated cleavage of viral transcripts (5).

The diverse silencing-suppression strategies reflect redundancy and functional specialization within plant sRNA pathways (4,5). *Arabidopsis* expresses at least three RNA-dependent RNA polymerases (RDR1, 2 and 6) thought to convert aberrant single-stranded RNA into dsRNA (6) and four Dicer-like (DCL) enzymes that process dsRNA or structured RNA into 21–24 nt sRNAs (1). RDR2 is required for the production of endogenous 24 nt, small-interfering RNA (siRNAs) that direct DNA methylation in plants (7). RDR6 generates

*To whom correspondence should be addressed. Tel: +41 61 2672977; Fax: +41 61 2673504; Email: Mikhail.Pooggin@unibas.ch
Present address:
Todd Blevins, Biology Department, Indiana University, Bloomington, IN, USA.

The authors wish it to be known that, in their opinion, the first two authors should be regarded as joint First Authors.

precursors for 21 nt *trans*-acting siRNAs that control the timing of organ development (1). During RNA virus infection, RDR1 and RDR6 have functions in the biogenesis or amplification of viral dsRNA (8–11), while DCL4 and DCL2 act to process this dsRNA into 21 nt and 22 nt vsRNAs, respectively (12). *Arabidopsis* mutants deficient for multiple DCL proteins are hypersusceptible to RNA viruses (12–14). The biogenesis of vsRNAs accompanying DNA virus infection is even more complex. In response to geminivirus infection, three *Arabidopsis* DCLs produce distinct size-classes of vsRNAs and during infection by the pararetrovirus *Cauliflower mosaic virus* (CaMV), four DCL enzymes are implicated, including DCL1 (14,15). DCL1 normally functions to excise plant miRNAs from hairpin RNA precursors. The particular mechanism of CaMV replication and structured RNA encoded in its genome may explain the involvement of all four DCLs (14,16).

The CaMV genome is transcribed into a more than genome length, 35S transcript in the nucleus by host RNA polymerase II (17). A shorter, 19S RNA transcript, co-terminal with the 35S RNA, is also produced during CaMV infection. It encodes the multifunctional transactivator/viroplasmin (TAV) protein, which is a weak silencing suppressor (18–20). The 35S RNA functions as both a polycistronic mRNA and as the template for reverse transcription (RT) required for viral genome replication (21). These functions are controlled by the 600 nt leader sequence that folds into an elongated hairpin (22–25). Interestingly, the leader region was previously identified as a rich source of vsRNAs (14,16).

We performed a global analysis of vsRNA populations in CaMV-infected *Arabidopsis* mutants and evaluated the impact of these vsRNAs on virus replication. Surprisingly, *dcl*-mutants that exhibit only minimal vsRNA accumulation did not show hypersusceptibility to CaMV infection. Massive vsRNA generation from the CaMV leader region, biased association of leader-derived vsRNAs with the AGO1 effector protein and the ability of this 600-bp non-coding sequence to confer enhanced infectivity to a chimeric geminivirus suggest that it plays a role in viral counter-defense.

MATERIALS AND METHODS

Arabidopsis mutant lines and virus infection

The *drd1-6*, *drd2-4*, and *drd3-7* (26), *nrpd2a-1* (27), *rdr2-1* (7) and *rdr6-15* (28) were described previously. Homozygous *rdr2 rdr6* was obtained in the F2 generation of a cross between *rdr2-1* and *rdr6-15*. Homozygous *rdr1 rdr2 rdr6* was obtained in the F2 generation of a cross between *rdr1-1* (7) and the abovementioned *rdr2 rdr6* line. Quadruple mutant *dcl1/2/3/4* material was obtained by crossing either *dcl1-8* (*sin1-2*) (29) or *dcl1-9* (*caf*) (30) to the triple mutant *dcl2/3/4* (14). *dcl1-9* used in the above crosses had been introgressed into Col-0 from Ler/Ws backgrounds by 5× outcrossing. After crossing *dcl1* to *dcl2/3/4*, F2 individuals of genotype *dcl1* (+/−) *dcl2* (−/−) *dcl3* (−/−) *dcl4* (−/−) were selected and self-fertilized. About 25% of resulting F3 progeny were quadruple homozygous.

Plant growth and inoculation with CaMV strain CM1841 were done as described previously (14). Infected plants were harvested 1-month post-inoculation, unless otherwise stated. Virus DNA titers were measured by semi-quantitative PCR as described (14) and by real-time quantitative PCR (qPCR) for viral DNA and qRT–PCR for polyadenylated viral RNAs. For qRT–PCR, cDNA was synthesized from 2 µg total RNA using 100 pmol of $d(T)_{16}$ primer. This mixture was heated to 70°C for 10 min and chilled on ice for 5 min. Then, the following reagents were added: 4 µl of 5× first-strand synthesis buffer [250 mM Tris–HCl (pH 8.3), 375 mM KCl, 15 mM $MgCl_2$, 0.1 M DTT], 2 µl 0.1 M DTT, 1 µl 10 mM dNTP mix and 1 µl (200 U) Superscript III reverse transcriptase (Invitrogen). The reaction was incubated at 50°C for 1 h and stopped by heating at 95°C for 5 min. One-tenth volume of the reaction mix was used for real-time PCR. Real-time PCR analysis with SYBR® Green (Applied Biosystems, UK) was carried out using the Applied Biosystems 7500 system. qPCR and qRT–PCR primers (Supplementary Table S3) specific for the virus (the CaMV leader and the TAV gene or the CaLCuV AC4 gene) and the internal control gene (ACT2 for qRT–PCR or 18S rDNA for qPCR) were designed using Beacon designer 2 software (PREMIER Biosoft International).

Small RNA analysis by Illumina sequencing

Total RNA was isolated from pools of three plants using the Trizol method as described previously (14). Ten micrograms of total RNA for each sample from mock-inoculated and CaMV-infected wild-type or mutant plants were taken for preparation of sRNA libraries following Illumina's modified protocol for the sRNA library construction kit. The 19–30 nt RNA fraction from total RNA samples was purified on a 15% TBE–Urea acrylamide gel. A 5′-adenylated single-stranded adapter was first ligated to the 3′-end of the RNA using T4 RNA ligase without ATP followed by a second single-stranded adapter ligated at the 5′-end of the RNA using T4 RNA ligase in the presence of ATP. The resulting products were purified on a 10% TBE–Urea acrylamide gel before performing the cDNA synthesis and PCR amplification. The resulting libraries were sequenced on an Illumina Genome Analyzer following the manufacturer's protocol.

After trimming the adaptor sequences, the datasets of all and unique reads were mapped to the reference genomes of *Arabidopsis thaliana* Col-0 (NCBI build 8.1) and CaMV (Genbank V00140) using the Mapping and Assembly with Qualities (MAQ) program (version 0.7.1) with a maximum of two mismatches to the reference sequences allowed. Reads mapping to several positions on the references with the same 'mapping quality' (i.e. number of mismatches and quality of the bases generating the mismatches) were attributed at random to one of them and attributed a 'zero' mapping quality. To account for the circular virus genome, reads that were not mapped on

the references were retrieved and mapped with the MAQ software on the viral junction, built from the last and first 50 bases of the viral sequence. The total reads that were mapped to the reference genomes with zero mismatches constituted upto ~90% in the libraries of a high coverage and quality run ('Col-0 mock', 'Col-0 CaMV', '*rdr1/2/6* CaMV' and '*dcl1-8* CaMV') and ~50% in the libraries of a lower coverage and quality run ('Col-0 CaMV*' and '*dcl2/3/4* CaMV*') and were taken for further analysis. For each reference genome and each sRNA size-class (20–25 nt), we counted once for all reads mapped and once for all reads mapped with a minimum quality of 10 (which implies uniquely mapped reads) the following: total number of reads, reads in forward and reverse orientation, reads starting with A, C, G and T (Supplementary Tables S1 and S2). In the single-base resolution maps of 20, 21, 22, 23, 24 and 25 nt vsRNA (Supplementary Data SD1), for each viral genome position we have displayed the number of matches starting at this position in reverse (last base of the read) and forward (first base of the read) orientations.

RNA blot hybridization

sRNA blot hybridization analysis was performed as in Blevins *et al*. (14) using short DNA oligonucleotide probes listed in Supplementary Table S3.

8S RNA mapping by cRT–PCR

Circularization reverse transcription–PCR (cRT–PCR) was carried out as described previously (31). Briefly, decapping was performed on 10 µg of total RNA using tobacco acid pyrophosphatase (Epicentre Technologies, Madison, WI, USA) in the presence of RNase inhibitor RNasin (Promega, Madison, WI, USA). After chloroform extraction, RNA was precipitated with ethanol and circularized using T4 RNA ligase 1 (NEB) in the presence of RNasin. Following extraction with chloroform, ligation products were precipitated with ethanol. Circular RNA was reverse transcribed using SuperScriptIII reverse transcriptase (Invitrogen) with either L94_as or L410_s primer (Supplementary Table S3). The cDNA synthesized with the L410_s primer was PCR amplified using *Taq* DNA polymerase (NEB) with the L410_s primer together with L13_as or L94_as primers and cDNA synthesized with the L94_as primer was PCR amplified with the L94_as primer together with L410_s or L514_s primers (Supplementary Table S3). PCR products were analyzed by agarose gel electrophoresis (Supplementary Figure S4), excised from the gel, cloned in pGEM-T Easy vector (Promega) and sequenced. In the cRT–PCR experiment performed without pyrophosphatase treatment, 10 µg of total RNA was directly taken for ligation, while other parameters remained the same.

Immunopurification of AGO proteins and associated sRNAs

This experiment followed an established protocol (32). Briefly, *Arabidopsis* tissue from mock-inoculated and CaMV-infected plants was ground in liquid nitrogen and incubated with ice-cold extraction buffer [50 mM Tris–HCl (pH 7.5), 300 mM NaCl, 10 mM $MgCl_2$, 0.5% NP-40, 5 mM dithiothreitol (DTT), complete protease inhibitor (Roche) and 10µM MG-132 (Sigma)] with agitation for 30 min at 4°C. Insoluble material was removed by centrifugation for 15 min at 15 300 rpm at 4°C. Lysate was pre-cleaned by incubation with 30 µl of protein A-agarose beads (Roche) at 4°C for 1 h. The 1 mL of supernatant was then incubated overnight at 4°C with either 5 µl of normal rabbit serum (NRS, Sigma), or 5 µl (5 µg IgG) of anti-AGO1 or anti-AGO4 sera (Agisera) pre-bound to 30 µl protein A-agarose beads. Immunoprecipitates were washed three times with the extraction buffer. Immunoprecipitated RNA was purified using the Trizol method and analyzed by RNA blot hybridization as described above. Aliquots of precipitated AGO proteins were analyzed by western blot.

Construction and testing of the CaLCuV-CaMV leader chimeric virus

The 612-bp CaMV leader fragment was PCR amplified with CamvL_Xho_s and CamvL_Xho_s primers (Supplementary Table S3), trimmed with XhoI (the site imbedded into each primer) and cloned into the XhoI site of the Cabbage leaf curl virus vector pMTCbLCVA.007 (33) in the antisense orientation. The resulting chimeric virus CaCLCuV-CamvL was tested for infectivity on *Arabidopsis* using biolistic delivery as described by Blevins *et al*. (14). As a control, we used the CaLCuV vector carrying a complete, green fluorescent protein (GFP) coding sequence of 714 bp inserted between KpnI and XhoI (CaLCuV-GFP). Accumulation of viral DNA in infected plants was measured by semi-quantitative PCR as described earlier (14) and confirmed by qPCR; for PCR primers see Supplementary Table S3. The vsRNAs derived from the CaMV and CaLCuV sequences were analyzed by RNA blot hybridization as described earlier (14) using DNA oligonucleotide probes (Supplementary Table S3).

RESULTS AND DISCUSSION

By ethidium bromide (EtBr) staining of size-separated RNA, we detected massive quantities of ~21–24 nt RNAs in CaMV-infected *Arabidopsis*. CaMV-derived sRNAs appeared to be more abundant in infected plants than the complement of host sRNAs detected in the mock-inoculated control (Figure 1A). In contrast, EtBr staining of RNA from *Cabbage leaf curl geminivirus* or *Oilseed rape mosaic tobamovirus* infections yielded scarcely detectable levels of sRNAs (data not shown). Abundant amounts of sRNAs were still detected in CaMV-infected plants deficient in DCL1, which is required for host miRNA biogenesis (*dcl1-8*, a hypomorphic mutant). They were also detected in infected plants deficient in RDR2, RDR6 or both RDR6 and RDR2 required for host siRNA biogenesis (null mutants *rdr2-1*, *rdr6-15* and double mutant *rdr2/6*) (Figure 1A). Thus, a large fraction of sRNAs detected by EtBr staining are likely to be vsRNAs of CaMV origin.

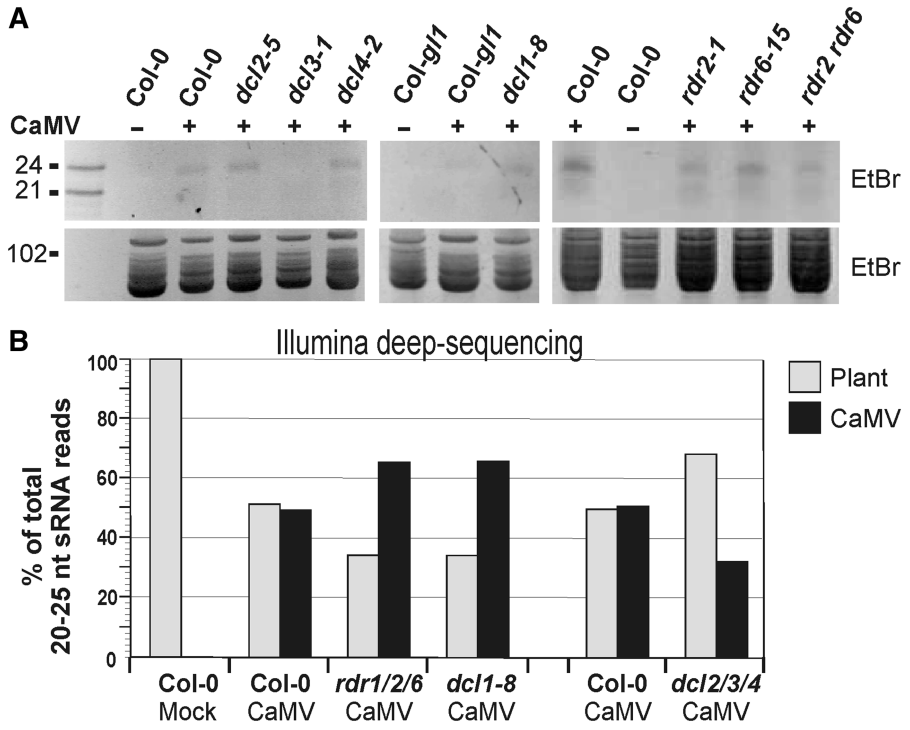

Figure 1. Massive, RDR-independent generation of CaMV vsRNAs in infected *Arabidopsis*. (**A**) Total RNA from pools of CaMV-infected (+) or mock-inoculated (−) wild-type control plants (Col-0 and Col-*gl1*) and mutants defective in host sRNA biogenesis: *dcl2-5*, *dcl3-1*, *dcl4-2*, *rdr2-1*, *rdr6-15* and *rdr2 rdr6* (all in Col-0) and *dcl1-8* (in Col-gl1). Plants were harvested 1-month post-inoculation or, in the case of *dcl1-8*, 2 months post-inoculation. Total RNA was separated by 15% PAGE and then stained with ethidium bromide (EtBr). Lower and upper portions of the gels are shown, the latter for RNA loading comparison. Positions of synthetic 21 and 24 nt RNA oligonucleotides and endogenous 102 nt U6 snRNA are indicated. (**B**) Illumina deep-sequencing of sRNAs from mock-inoculated and CaMV-infected *Arabidopsis* wild-type (Col-0) and mutants (*rdr1/2/6*, *dcl1-8* and *dcl2/3/4*) confirms massive production of RDR-independent vsRNA, comparable to the entire complement of host sRNAs. The graph shows the percentage of *Arabidopsis* and vsRNAs in the pool of 20–25 nt reads mapped to the *Arabidopsis* and CaMV genomes with zero mismatches.

The 24-nt sRNA signal was abolished in the null mutant *dcl3-1*, confirming that the biogenesis of this size-class of viral and host sRNAs is DCL3 dependent (7,14).

To survey genome-wide interactions of CaMV with the plant RNA silencing machinery we sequenced sRNA populations from virus-infected wild-type and mutant plants using Illumina technology (www.illumina.com). The procedure selected for sRNAs with 5′-phosphate and 3′-hydroxyl groups, i.e. DCL activity products. Consistent with earlier reports (34,35), 81% of the 549 540 sRNA reads from mock-inoculated seedlings fell into the 20–25 nt range, of which 75% mapped to the *Arabidopsis* genome with zero mismatches; 24 nt and 21 nt reads were predominant (Figure 2A and Supplementary Table S1). Likewise, 81% of the 1 470 760 reads from CaMV-infected plants fell into the 20–25 nt range, of which 40% mapped perfectly to the *Arabidopsis* genome (~120 Mb) and 39% mapped perfectly to the CaMV genome (~8 kb) (Figure 1B, Supplementary Table S1). Among 20–25 nt vsRNAs, the 24 nt fraction was largest (47%), while the 21 and 22 nt fractions were second (27%) and third (14%) largest in abundance (Figure 2B), respectively. This size-class distribution agrees with our results for the relative abundance of CaMV-derived sRNAs detected by blot hybridization (14). To summarize the gel analysis and sequencing data are in agreement and show that the vsRNA pool is comparable in size to the entire complement of host miRNAs and siRNAs.

To investigate whether CaMV vsRNAs are redundantly amplified by RDR activities known to mediate sRNA biogenesis (6), we generated a triple null mutant *rdr1 rdr2 rdr6* (*rdr1/2/6*) and sequenced sRNAs from infected *rdr1/2/6* plants. In *rdr1/2/6*, 20–25 nt sRNAs perfectly matching the CaMV genome represented 54% of 748 199 reads, while those perfectly matching the *Arabidopsis* genome only represented 28% of the reads (Supplementary Table S1 and Figure 1B). The decreased percentage of host sRNAs in this mutant compared with the wild-type resulted from a 10-fold decrease in RDR2-dependent 24 nt sRNAs. In contrast to the profile for host sRNAs, the profile for vsRNAs did not change significantly in *rdr1/2/6* relative to wild-type (Figure 2B and Supplementary Table S1). From this, we conclude that at the late stage of infection, CaMV-derived vsRNAs are largely produced independently of RDR1, RDR2 and RDR6. We cannot, however, exclude that CaMV vsRNAs can potentially be amplified by these RDRs at the earlier stages of infection or under certain conditions. In RNA virus infections of *Arabidopsis*, vsRNAs are amplified by

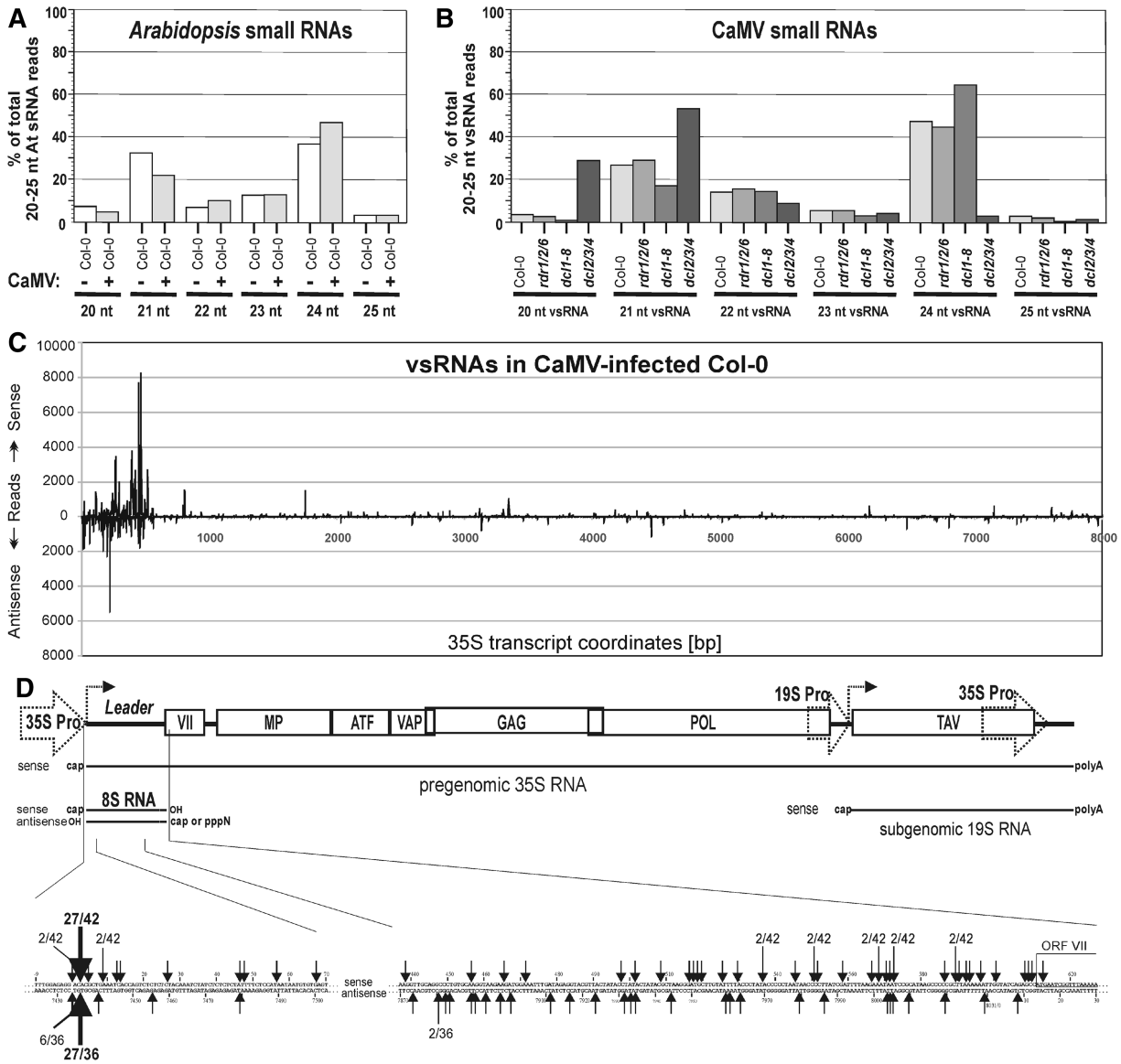

Figure 2. Illumina deep-sequencing analysis of CaMV sRNAs and comparative mappings of viral RNA molecules. Bar graphs showing the percentages of (**A**) *Arabidopsis* sRNAs and (**B**) vsRNAs in the pool of 20–25 nt sRNA reads sequenced from CaMV-infected wild-type (Col-0) and mutant lines (*rdr1/2/6*, *dcl1-8* and *dcl2/3/4*)—for number of reads, see Supplementary Table S1. (**C**) Genome-wide map of vsRNAs from CaMV-infected Col-0 at single-nucleotide resolution. The graph plots the number of 20–25 nt vsRNA reads at each position of the 8031-bp CaMV genome; the numbering starts at the 5′-terminus of the 35S RNA (genome position 7434) as depicted in panel D. Bars above the axis represent sense reads starting at each respective position; those below represent antisense reads ending at the respective position (Supplementary Data). (**D**) cRT–PCR mapping of CaMV 8S RNA from virus-infected *Arabidopsis* (Supplementary Figure S4 for experimental details). The circular CaMV genome organization is shown schematically with viral genes (boxes) and 35S and 19S promoters (dotted arrows) that drive Pol II transcription of two major transcripts: the pregenomic 35S RNA and subgenomic 19 RNAs (depicted below the genome). The position and termini of the CaMV leader region-derived 8S RNA species are indicated, as determined for sense and antisense polarities by cRT–PCR product sequencing. Regions surrounding the 35S RNA start site and the 3′-terminal part of the leader sequence preceding ORF VII are enlarged. The termini of sequenced 8S RNA clones are indicated by arrows above the sequence for sense RNAs (42 clones) and below the sequence for antisense RNAs (36 clones). The number of clones is given when more than one clone had the same 5′- or 3′-terminus. Thick arrows indicate the major transcription start site for sense 8S RNAs and the major 3′-terminus for antisense 8S RNAs, which fall on the same genome position.

RDR1 and/or RDR6; this amplification becomes most evident when a viral silencing suppressor gene is inactivated (8–11). The ability of the CaMV TAV protein to interfere with host RDR6-dependent sRNA pathways (19,20) could account for the lack of RDR6-dependent vsRNAs in CaMV-infected plants. Likewise, TAV may also inhibit production of RDR1-dependent vsRNAs. It would be interesting to investigate whether a CaMV mutant deficient for the silencing suppressor activity of TAV can generate RDR-dependent vsRNAs. However, the suppressor activity would first need to be genetically uncoupled

from other TAV functions that are essential for viral replication.

We also sequenced sRNAs from a hypomorphic mutant deficient for DCL1 (*dcl1-8*). In CaMV-infected *dcl1-8*, viral reads outnumbered *Arabidopsis* genome-derived reads due to the reduction in host miRNA accumulation (Figure 1B and Supplementary Table S1). Of 20–25 nt vsRNAs in *dcl1-8*, the fraction of 21 nt reads (17%) was significantly lower than that in wild-type plants (27%) (Figure 2B). This confirms our earlier finding that DCL1 contributes to the biogenesis of 21 nt vsRNAs (14). The role of DCL1 in vsRNA biogenesis is also supported by the sRNA sequence profiles we obtained for CaMV-infected *dcl2 dcl3 dcl4* triple null mutant (*dcl2/3/4*) plants. The relative levels of 22 and 24 nt vsRNAs were drastically reduced, whereas the relative level of 21 nt vsRNA was increased compared to wild-type plants (Figure 2B and Supplementary Table S1).

The distribution of 20–25 nt vsRNA reads across the 8031-bp CaMV genome was plotted at the single-nucleotide scale (Figure 2C, Supplementary data SD1, Supplementary Figures S1 and S2). These maps show a biased distribution in terms of strand orientation and position. First, 62% of reads from infected wild-type plants matched the viral transcript polarity (i.e. sense polarity). The sense-strand bias was also observed in the mutant lines (Supplementary Table S1 and Supplementary Figure S1). Second, both in wild-type and mutant plants, a majority of viral reads, 65–82%, aligned to the ~600-bp leader region (Figure 2C, Supplementary Figure S1 and Supplementary Table S1). Leader-specific reads are distributed unevenly: several 50–80 nt 'hot spots' give rise to most vsRNAs of either polarity. We found no correlation of these hot spots with strong and regular secondary structures compatible with DCL binding and processing. If unique vsRNA sequences are considered (Supplementary Table S2), they densely tile across the entire leader region in both polarities (Supplementary Figure S2). Within hot spots, almost every nucleotide position marks the 5′-end of 21, 22 and 24 nt species, each represented with up to several thousand reads (Supplementary Figure S2 and Supplementary data SD1). Similar hot spots were found in independent samples from wild-type plants and in samples from *rdr1/2/6* and *dcl2/3/4* plants. In *dcl1-8*, the hot spots were shifted slightly (Supplementary Figures S1 and S2 and Supplementary data SD1). Thus, in the absence of a fully functional DCL1, other DCLs process vsRNA precursors with somewhat altered sequence specificity.

We validated the deep-sequencing data by RNA blot hybridization using 36-short DNA oligonucleotide probes specific to CaMV (Supplementary Table S3) and confirmed a reproducible pattern of vsRNA hot spots covering the leader region in both polarities (Supplementary Figure S3). Both approaches reveal the hot spots in the same zones within the leader region. In contrast, only very low levels of vsRNAs could be detected with probes specific to the 35S promoter region upstream of the leader (Supplementary Figure S3), which also agrees with our deep-sequencing data (Supplementary data SD1). Genetic requirements for vsRNA biogenesis were found to be similar throughout the leader region (Supplementary Figure S3). Together, our blot hybridization and sequencing data indicate that each of the four DCLs processes a leader-length dsRNA precursor or, alternatively, multiple overlapping dsRNAs derived from the entire leader. This dsRNA processing appears to be initiated internally and sporadically, but with some preference for the hot spots. It is also possible that differential vsRNA stability contributes to hot spot formation. No phasing could be discerned that would resemble processing of *trans*-acting siRNAs from RDR6-dependent dsRNA (28).

The robust systemic infection and viral DNA accumulation that we observed in spite of massive vsRNA production was surprising. In the case of RNA viruses, strong suppressor proteins such as a potyviral HC-Pro are known to inactivate vsRNAs (5,11). However, this is not sufficient to explain our observations for CaMV, which does not encode a strong suppressor protein. The CaMV TAV protein is a weak silencing suppressor that perturbs RDR6-dependent pathways associated with sRNA amplification (18–20). Furthermore, CaMV infection does not suppress transgene silencing triggered by RDR6-independent dsRNA (20). To test whether massively produced CaMV vsRNAs have an antiviral function, we generated two *dcl1 dcl2 dcl3 dcl4* (*dcl1/2/3/4*) quadruple mutants each carrying a hypomorphic allele of *DCL1* (*dcl1-8* or *dcl1-9*) and null alleles of *DCL2*, *DCL3* and *DCL4*. RNA blot hybridization showed that, compared to triple mutant *dcl2/3/4*, both quadruple mutants accumulated only residual 21 nt vsRNAs (Figure 3A and Supplementary Figure S3). The truncated DCL1 protein encoded by *dcl1-9* mutant alleles can process miRNA precursors, but less efficiently and precisely than wild-type DCL1 (36). This leads to destabilization of most miRNAs, including miR173 but excluding miR168 (37): we used these two miRNAs as controls (Figure 3A).

RNA viruses have been shown to accumulate at higher levels in *dcl1/2/3/4* plants (13). In contrast, titers of CaMV DNA and polyadenylated 35S and 19S transcripts were not affected substantially in *dcl1/2/3/4* or *dcl2/3/4* as measured by real-time qPCR and qRT–PCR, respectively (Figure 3B), and by other methods (Supplementary Figure S4). This extends our finding that CaMV DNA accumulation is not dramatically affected in any of the four single *dcl* mutants (14), and is in contrast to Moissiard and Voinnet (16) who observed a strong increase in accumulation of CaMV 35S RNA and coat protein in *dcl2/3/4* compared to wild-type plants. The fact that distinct strains of CaMV were studied—CM1841 in our case and JI in (16)—may account for this discrepancy. In different CaMV strains, the TAV protein is known to be a determinant of host range and symptom severity. TAV function in suppressing RNA silencing-based host defenses may also be strain dependent.

Stability and function of *Arabidopsis* sRNAs depend on their incorporation into an RNA-induced silencing complex (RISC) through binding to AGO proteins that sort sRNAs based on their 5′-nt and size (38–40). Thus, a majority of 21 nt miRNAs have 5′ uridine (5′U)-termini and associate with AGO1, whereas a large fraction of

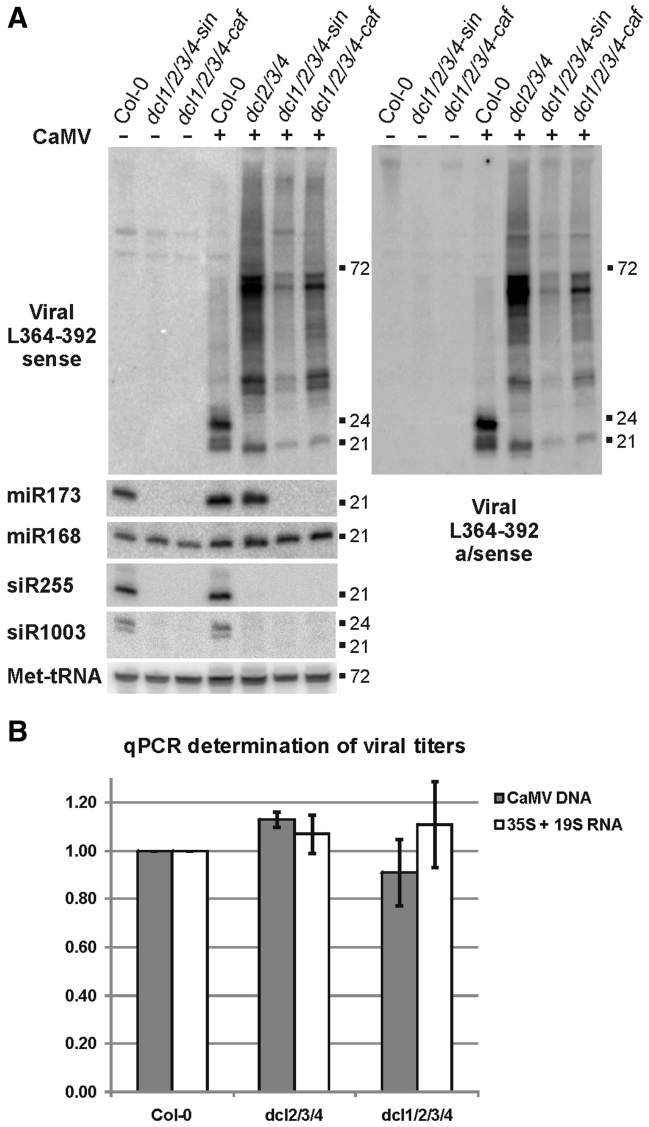

Figure 3. CaMV vsRNAs and DNA/RNA titers detected in quadruple *dcl*-mutants. (**A**) Analysis of low-molecular weight RNA extracted from pools of CaMV-infected (+) or mock-inoculated (−) plants: wild-type (Col-0), triple *dcl*-mutant (*dcl2/3/4*) and two quadruple *dcl*-mutants carrying weak *dcl1* alleles (*dcl1/2/3/4-sin*, *dcl1/2/3/4-caf*). Size-fractionated RNA was analyzed by 18% PAGE followed by blot hybridization. The membrane was successively hybridized with sense and antisense DNA oligonucleotide probes for the CaMV leader region, and probes for host sRNAs: miR173 (22 nt), miR168 (21 nt), siR255 (21 nt), siR1003 (24 nt). Met-tRNA (72 nt) serves as a loading control. Sizes are indicated on each data image. (**B**) Viral titers in CaMV-infected wild-type (Col-0), *dcl2/3/4* and *dcl1/2/3/4-caf* were measured using quantitative real-time PCR (qPCR) for viral DNA and qRT–PCR for polyadenylated 35S and 19S transcripts (see 'Materials and Methods' section). In both cases, PCR primers specific for the CaMV leader-region and the CaMV TAV region (Supplementary Table S3) were used in parallel for each sample. As internal controls, we performed qPCR and qRT–PCR on the same DNA and cDNA samples with primers specific for 18S rDNA and ACT2 gene, respectively (Supplementary Table S3). The mean of the normalized levels for viral DNA and RNA (the sum of 35S and 18S RNAs) is shown; the CaMV titer in wild-type (Col-0) plants was set to one in each case.

24 nt siRNAs have 5′ adenosine (5′A)-termini and associate with AGO4. In line with this, in our data sets, we found that 21 nt host sRNAs predominantly have 5′U (78% of the total 21 nt reads; Supplementary Table S1), whereas 24 nt host sRNAs predominantly have 5′A (60% of the total 24 nt reads). In contrast, 29% of 21 nt viral sRNAs have 5′U-termini and 41% have 5′A-termini (Supplementary Table S1), which would predict their association with AGO1 and AGO2, respectively (37). We previously observed an up-regulation of *AGO2* and *AGO7* but not other *AGO* genes in CaMV-infected plants (20). Because AGO7 interacts specifically with miR390 (39), increased availability of AGO2 protein is more likely to account for preferential accumulation of 5′A vsRNAs. AGO2 binds vsRNAs derived from *Cucumber mosaic virus*, which is an RNA virus (40), but no functions of AGO2 in antiviral defense or silencing of host genes are known.

In principle, CaMV derived 24 nt vsRNAs with 5′A-termini (35% of the total 24 nt reads; Supplementary Table S1) could associate with AGO4 to mediate viral DNA methylation. In addition to AGO4, the host siRNA-directed *de novo* methylation pathway depends on the RNA polymerases Pol IV and Pol V and the chromatin remodeling factor DRD1 (26,41). Our earlier studies showed that deficiencies in AGO4 and Pol IV do not affect CaMV DNA accumulation and only slightly affect vsRNA accumulation (14); we confirmed this result here using *drd2-4*, a different loss-of-function mutant for Pol IV (Supplementary Figure S5). Similarly, we did not find drastic changes in CaMV DNA and vsRNA accumulation caused by deficiencies in Pol V or DRD1 (*drd3-7* and *drd1-6*, respectively) (Supplementary Figure S5). These findings and the fact that CaMV DNA is actively transcribed throughout the infection cycle (42) strongly suggest that the *de novo* methylation pathway is not a major player in CaMV silencing. In line with this, we found very little vsRNAs derived from the 35S promoter region in CaMV-infected plants (Supplementary Figure S3 and our Illumina data). Moreover, only negligible amounts of leader-derived vsRNAs and no vsRNAs from promoter and coding regions were detected bound to the AGO4 protein in our immunoprecipitation (IP) assay with native antibodies for AGO4 (Supplementary Figure S5).

The massive production of vsRNAs of both polarities from the 35S RNA leader region suggests that sense and antisense transcripts covering just this region could be their precursors. Such sense RNA was described earlier as a viral 8S RNA of unknown function (17). By using cRT–PCR (31), we isolated multiple species of 8S RNA from CaMV-infected wild-type or *dcl2/3/4 Arabidopsis* plants (Figure 2D and Supplementary Figure S6). The 8S RNA starts at either of two consecutive AC-motifs, the first of which was reported as the common start site of 35S and 8S RNAs (17), but ends heterogeneously close to the primer binding site of RT located at the end of the leader sequence (Figure 2D). At this position, the virion CaMV DNA has a discontinuity of the minus (antisense) strand marking the start and the end of RT (21). Abrupt termination of 35S promoter-directed transcription close

to the discontinuity of the unsealed DNA template in the nucleus might lead to accumulation of sense 8S RNA. Alternatively, sense 8S RNA that folds into an extended hairpin structure (see below) may be processed from 35S RNA by 'Drosha'-like activity of DCL1 (36) as suggested previously (16).

Using cRT–PCR with reverse primers, we found multiple antisense copies of 8S RNA. These antisense transcripts start around the positions of the 3′-ends of sense 8S RNAs and end precisely at the sense 8S RNA start site, essentially mirroring sense 8S RNAs (Figure 2D and Supplementary Figure S6). We propose that sense and antisense 8S RNAs form dsRNAs that are then processed by DCLs to generate vsRNAs. Both sense and antisense 8S RNAs lack a poly(A) tail and are sensitive to pyrophosphatase (Supplementary Figure S6), suggesting that they are either capped or 5′-triphosphorylated. The heterogeneity of the 5′-termini and the lack of adequately positioned promoter consensus sequences in antisense orientation argue against production of antisense 8S RNA on a CaMV DNA template. On the other hand, our mapping data are consistent with a model, in which 8S RNA sense transcripts are converted into dsRNAs by an RNA-directed RNA polymerase activity. This polymerase would drop off at the 5′-end of the template without adding extra non-template nucleotides. Our genetic evidence excludes RDR1, RDR2 and RDR6 as well as Pol IV and Pol V as this enzyme, because wild-type amounts of CaMV leader-derived vsRNAs of both polarities accumulated in *rdr1/2/6* (see above) as well as in the loss-of-function mutants for Pol IV [(14), (Supplementary Figure S5; *drd2-7* and *nrpd2a-1*)] and Pol V (Supplementary Figure S5; *drd3-7* and *nrpd2a-1*). Formally, we cannot exclude a possibility that three additional genes of the *Arabidosis* RDR family, for which no function was reported so far (6), may be involved. Another, more likely, candidate would be Pol II. Pol II is known to replicate animal hepatitis delta virus and plant RNA viroids, circular single-stranded RNAs that form extensive secondary structures (43). The CaMV leader sequence forms such a viroid-like structure (23). Furthermore, Lipardi and Paterson (44) have reported that the largest subunit of *Drosophila* Pol II has an RDR activity and participates in RNA silencing and transposon suppression.

Despite the hindrance to translation initiation on viral 35S RNA due to the presence of a highly structured leader, the approximate size and secondary structure, but not the primary sequence of the leader region are highly conserved in diverse plant pararetroviruses (45). Furthermore, most mutations and second site reversions in the CaMV leader primary sequence have little effect on virus replication (25,46,47). These considerations and the fact that a complex shunt mechanism has evolved to allow scanning ribosomes to bypass the leader (22,25,45) suggest that there is a selective advantage for a long, highly structured leader.

One possibility is that the complexity and length of the leader are required for the function of polyadenylation, packaging and splicing signals that it contains; but, this seems unlikely because these signals require much less space and structure in other DNA viruses. Another possibility is that the vsRNAs produced from the leader region play a role in viral counter-defense. Moissiard and Voinnet (16) have proposed that the CaMV leader forms a miRNA precursor-like structure and some leader-derived vsRNAs target host genes in a sequence-specific manner to the advantage of the virus. Our transcriptome profiling of CaMV-infected plants and of transgenic plants expressing CaMV TAV protein (20) revealed only modest downregulation of some predicted target genes, which appears to depend on CaMV TAV expression rather than vsRNAs *per se* (Supplementary Figure S7). The fact that the leader primary sequence is not evolutionary conserved also argues against a sequence-specific role for leader-derived vsRNAs in viral counter-defense.

More consistent with our data is a hypothesis that the 8S duplex RNA derived from the leader region acts as a silencing decoy to engage all four DCLs in massive production of vsRNAs. These highly abundant vsRNAs could prevent less abundant vsRNAs produced from other CaMV genome regions from being assembled into AGO–RISCs. Our finding that CaMV titers are not affected in the *dcl1/2/3/4* mutants, in which both the host defense and the viral leader-based counter-defense are undermined, indicates that sporadic production of vsRNAs outside of the leader region does not contribute substantially to restricting virus replication. Thus, in the wild-type plants, these less abundant vsRNAs do not appear to form sufficient amounts of active AGO–RISCs to silence viral transcripts. To test this hypothesis, we analyzed vsRNAs associated with AGO1, the major AGO effector protein implicated in antiviral defense (48–51). IP of AGO1 from CaMV-infected plants with a specific native antibody (49) yielded a sample highly enriched with leader-derived vsRNAs, whereas vsRNAs derived from other CaMV genome regions were not detected (Figure 4).

AGO–RISCs charged with leader-derived vsRNAs of antisense polarity could potentially target 35S RNA. However, the leader sequence of 35S RNA forms a stable secondary structure required for both translation (25,47) and packaging/RT (24) and this structure would prevent RISC binding. In line with this, our previous studies indicate that stability and integrity of the leader secondary structure correlates with CaMV infectivity (25,46,47). Studies of viroids and viral satellites and defective-interfering RNAs have shown that although vsRNAs can be produced from such precursors (presumably during replication when they spawn dsRNAs), their secondary structures largely prevent them from being targeted by the resulting vsRNAs (10,52–55).

Massively produced vsRNAs could potentially compete with host miRNAs and siRNAs for free AGO proteins, interfering with endogenous RISC function. But our AGO-IP experiments do not support this idea: binding of miR173 to AGO1 and the AtREP2 siRNAs to AGO4 was not perturbed by CaMV infection (Figure 4 and Supplementary Figure S5). Accordingly, our previous study indicates that CaMV infection and CaMV TAV expression do not interfere with miR173-directed cleavage of

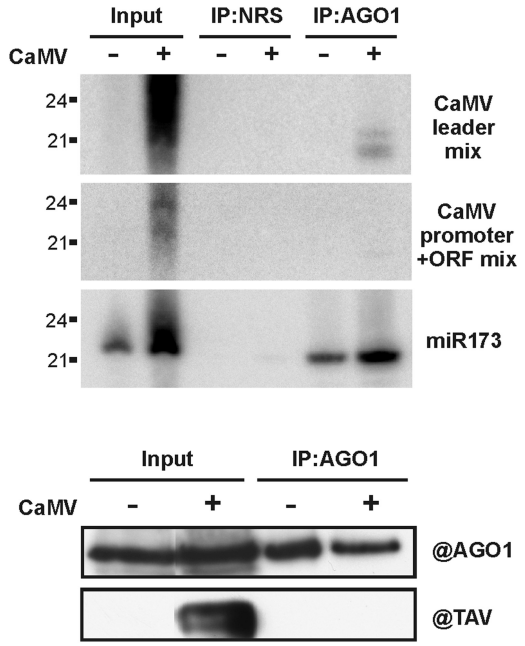

Figure 4. Preferential loading of CaMV leader-derived vsRNAs into AGO1 and the effect of CaMV infection on accumulation of AGO1 protein and AGO1-associated miRNA. The upper panel shows RNA blot hybridization analysis of total sRNAs (input) and sRNAs associated with AGO1 protein in mock-inoculated (−) or CaMV-infected (+) plants following immunoprecipitation with AGO1-specific antibodies (IP:AGO1) or normal rabbit serum (IP:NRS) as a negative control. The membrane was successively hybridized with mixtures of non-overlapping sense and antisense DNA probes specific for the CaMV leader region (CaMV leader mix) or the CaMV 35 promoter and ORF VII/I regions (CaMV promoter + ORF mix) and the probe specific for miR173 (22 nt) (Supplementary Table S3). The lower panel shows western blot analysis of AGO1 protein accumulation in the input and the IP:AGO1 fractions using AGO1-specific antibodies (@AGO1). The blot was also stained with antibodies specific for CaMV TAV protein (@TAV).

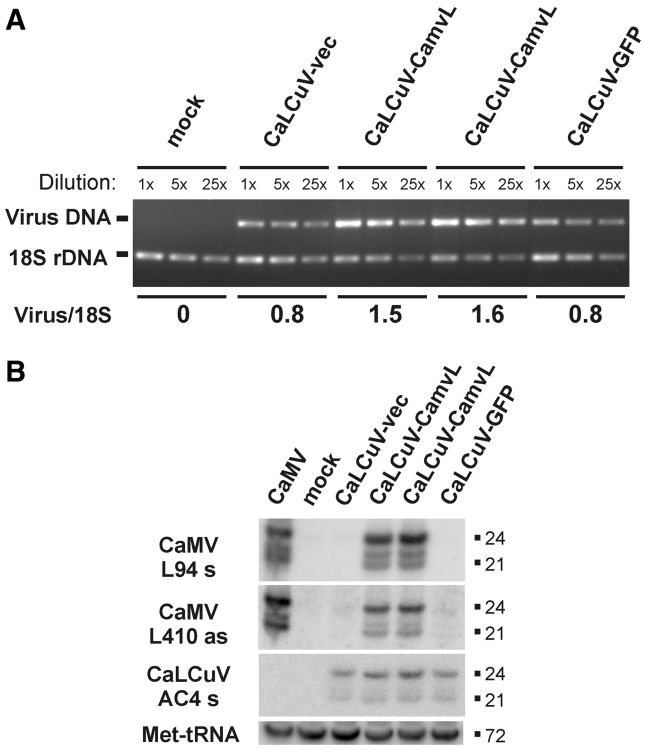

Figure 5. Ectopic expression of CaMV leader-derived vsRNAs from an attenuated geminivirus slightly increases viral DNA accumulation. (**A**) Viral DNA titers in *Arabidopsis* plants infected with a CaLCuV vector carrying the CaMV leader sequence (CaLCuV-CamvL) versus the vector control virus (CaLCuV-vec) or the vector carrying a non-viral insert (CaLCuV-GFP) were measured by semi-quantitative PCR on serial dilutions (5-fold each) of total DNA isolated from pools of three to four infected or mock-inoculated plants. 18S ribosomal DNA amplification is an internal control. The titers were also confirmed by qPCR. (**B**) vsRNAs were analyzed by RNA blot hybridization using total RNA from pools of three to four virus-infected (CaMV, CaLCuV-vec, CaLCuV-CamvL and CaLCuV-GFP) or mock-inoculated plants. The membrane was successively hybridized with DNA oligonucleotide probes for the CaMV leader region and CaLCuV AC4 gene. Met-tRNA is shown as a loading control. Note that two independent clones of the CaLCuV-CamvL construct were analyzed.

target transcripts (20). Moreover, our transcriptome profiling did not reveal a general upregulation of miRNA-targeted transcripts upon CaMV infection, except for those silenced by RDR6-dependent secondary siRNAs; the latter effect is attributable to the silencing suppressor activity of CaMV TAV protein (20). Thus AGO-RISCs programmed by host miRNAs and siRNAs do not appear to be perturbed by massive production of vsRNAs. Therefore, leader-derived 8S dsRNA/vsRNAs cannot be considered as a general decoy that interferes with all RNA silencing pathways. Instead, massive production of vsRNAs from the leader region may divert the silencing machinery from targeting the most vulnerable CaMV regions, i.e. viral promoters and unstructured coding regions of 19S and 35S transcripts.

The CaMV leader-based *cis*-elements and structures are essential for viral replication and therefore the leader sequence cannot be deleted from or replaced by a heterologous leader in CaMV genome without drastically affecting CaMV infectivity (25,46,47). To provide further evidence for our decoy hypothesis, we therefore expressed leader-derived vsRNAs ectopically from a heterologous DNA virus. We made use of an attenuated geminivirus, *Cabbage leaf curl virus* (CaLCuV), lacking the coding sequence of its coat protein gene (33). The CaMV leader sequence was inserted between the CaLCuV Pol II promoter and terminator in place of the coat protein gene. If massively produced leader-derived vsRNAs would be antiviral, infectivity and DNA accumulation of the resulting chimeric virus should be reduced. In contrast, the chimeric virus exhibited increased infectivity on *Arabidopsis* and accumulated measurably higher DNA titers than the CaLCuV vector control or the vector carrying a non-viral insert of similar length (green fluorescent protein gene sequence of 714 bp; GFP) (Figure 5A). Plants infected with the CaLCuV::CaMV leader chimera accumulated high levels of 21–24 nt vsRNAs from the inserted CaMV leader region, which were comparable to the levels of leader-derived vsRNAs accumulating in

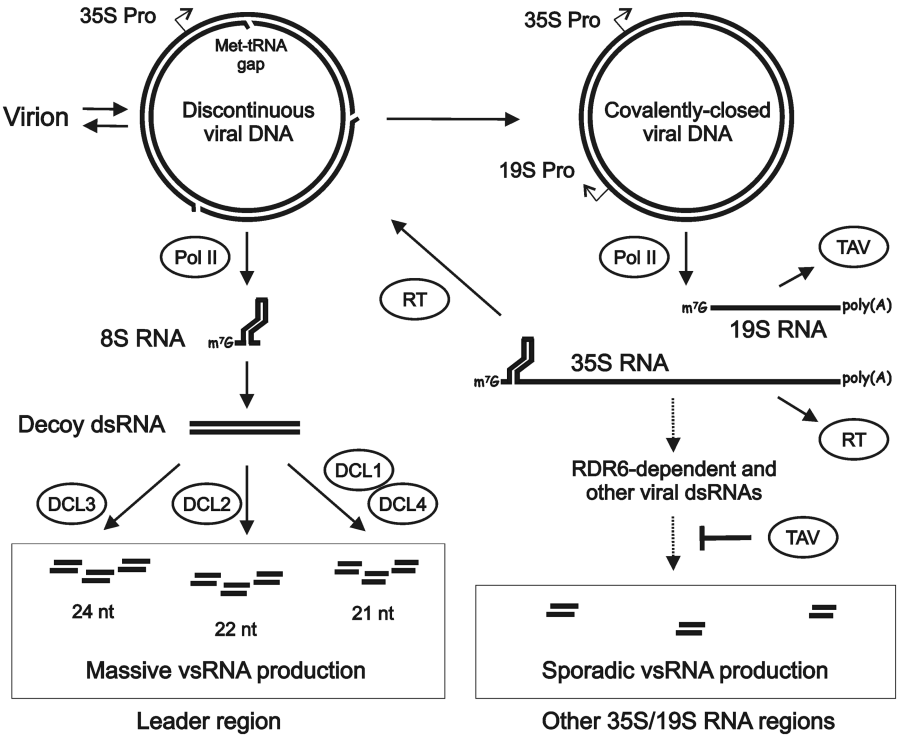

Figure 6. Model for CaMV interactions with the *Arabidopsis* sRNA-generating machinery. Viral DNA is released from the virion into the nucleoplasm. Gaps in this DNA left by RT during the previous replication cycle are repaired by host DNA repair enzymes to create covalently closed molecules. Closed viral DNA is transcribed by Pol II into pregenomic 35S RNA, which is a polycistronic mRNA for several viral proteins including RT and a template for RT. Viral DNA is also transcribed by Pol II into subgenomic 19S RNA, which is the mRNA for the viral transactivator/viroplasmin protein (TAV). Abrupt termination of Pol II-driven transcription, potentially caused by an unrepaired DNA gap (Met-tRNA gap), results in production of aberrant 8S RNAs lacking poly(A) tails. This 8S RNA matches the 35S RNA leader sequence, and is predicted to form a viroid-like secondary structure, which may be converted to dsRNA by Pol II. We hypothesize that 8S RNA-derived dsRNA serves as a decoy to engage all four DCLs in massive production of 21, 22 and 24 nt vsRNAs. These leader-region vsRNAs would compete with vsRNAs derived from other regions for AGO proteins. Resulting antisense vsRNAs would potentially guide AGO-meditated silencing of 35S RNAs, but the structured nature of the leader would likely hinder vsRNA pairing. Sporadic cleavage products of 35S or 19S RNA enter sRNA biogenesis pathways (evidenced by low-level vsRNA biogenesis from these regions), but host RDR6-dependent processes are suppressed by viral TAV protein (19,20).

CaMV-infected plants (Figure 5B). VsRNAs from the CaLCuV genome also accumulated, albeit at lower levels (Figure 5B). The accumulation of the CaLCuV genome-specific vsRNAs from the CaLCuV::CaMV leader chimeric virus was slightly higher than for the case of the CaLCuV empty vector and CaLCuV::GFP control virus, which correlates with their respective viral DNA titers. Thus, despite the production of CaMV leader-derived vsRNAs in addition to CaLCuV-specific vsRNAs, replication of the chimeric virus was not reduced. These data are consistent with our decoy hypothesis.

CONCLUSIONS

Here, we demonstrate that CaMV infection is associated with massive production of RDR1-/RDR2-/RDR6-independent vsRNAs from the leader region, whereas other regions of the viral genome spawn only low amounts of vsRNAs. The quantity of leader-derived vsRNAs is comparable to the entire complement of endogenous plant miRNAs and siRNAs. Illumina sequencing of vsRNAs revealed several hot spots matching both polarities of the leader region. Likely precursors of these vsRNAs are long double-stranded molecules arising from Pol II transcription of the entire leader region into sense and antisense 8S RNAs, which we detected by cRT–PCR. Genetic evidence indicates that all four DCLs process vsRNAs from their precursors. This processing occurs internally with some preference for hot spot sequences, but differential vsRNA stability may also account for hot spot formation.

CaMV titers were not elevated in *dcl*-quadruple mutants, despite vsRNA levels being greatly diminished. Thus, massive vsRNA production in wild-type plants does not appear to restrict viral replication. Furthermore, ectopic expression of CaMV leader vsRNAs from an attenuated geminivirus did not render the chimeric virus more prone to plant antiviral defenses. These results raise the possibility that in addition to expressing the silencing suppressor protein TAV that interferes with RDR-dependent amplification of siRNAs (18–20), CaMV deploys counter-defense based on decoy 8S dsRNA generated from the non-coding leader region (Figure 6). Massive production of primary vsRNAs from 8S dsRNA might divert silencing effectors from targeting CaMV promoters and unstructured transcripts outside of the leader region. AGO1 is a major effector of antiviral silencing in

plants, which explains why RNA viruses express suppressor proteins that target AGO1 for degradation, reduce AGO1 protein translation, or disrupt its RNA cleavage activity (5,48–51). Unlike RNA viruses, CaMV infection did not perturb AGO1 accumulation, its association with endogenous miRNAs or activity. The fact that leader-derived vsRNAs were associated with AGO1, whereas vsRNAs from other regions of CaMV genome were not detected in the AGO1 complexes, lends further support to our decoy model of CaMV counter-defense (Figure 6).

It will be interesting to explore whether other plant viruses use decoy RNAs to evade silencing. Studies on human adenovirus found that highly structured viral RNAs suppress the interferon-mediated antiviral defense and sequester Dicer (56). Thus an RNA decoy strategy to counteract antiviral defense may be common among plant and animal viruses.

SUPPLEMENTARY DATA

Supplementary Data are available at NAR Online.

ACKNOWLEDGEMENTS

We thank Nachelli Malpica and Ekaterina Gubaeva for technical assistance, Marjory Matzke for seeds of *drd1-6*, *drd2-4* and *drd3-7* and Craig Pikaard for supporting part of T.B.'s experiments; and the Novartis Research Foundation for supporting work done at the Friedrich Miescher Institute. We are grateful to Thomas Boller, Andres Wiemken and Christian Körner for hosting the group at the Botanical Institute. T.B. and M.M.P. designed research, T.B., R.R., M.A., M.S. and B.K.B. performed research. L.B., L.F., T.B., T.H. and M.M.P. analyzed data, T.B., F.M., T.H. and M.M.P. wrote the article.

FUNDING

Swiss National Science Foundation grants (31003A_122469 to T.H. and M.M.P., 31003A_127514 to M.M.P.); European Molecular Biology Organization (EMBO short term fellowship ASTF 169.00-2010 to M.S.); European Commission (a Marie Curie fellowship PIIF-237493-SUPRA to R.R.). Funding for open access charge: Friedrich Miescher Institute.

Conflict of interest statement. None declared.

REFERENCES

1. Chapman,E.J. and Carrington,J.C. (2007) Specialization and evolution of endogenous small RNA pathways. *Nat. Rev. Genet.*, **8**, 884–896.
2. Ruiz-Ferrer,V. and Voinnet,O. (2009) Roles of plant small RNAs in biotic stress responses. *Annu. Rev. Plant Biol.*, **60**, 485–510.
3. Hamilton,A.J. and Baulcombe,D.C. (1999) A species of small antisense RNA in posttranscriptional gene silencing in plants. *Science*, **286**, 950–952.
4. Ding,S.W. and Voinnet,O. (2007) Antiviral immunity directed by small RNAs. *Cell*, **130**, 413–426.
5. Csorba,T., Pantaleo,V. and Burgyán,J. (2009) RNA silencing: an antiviral mechanism. *Adv. Virus Res.*, **75**, 35–71.
6. Wassenegger,M. and Krczal,G. (2006) Nomenclature and functions of RNA-directed RNA polymerases. *Trends Plant Sci.*, **11**, 142–151.
7. Xie,Z., Johansen,L.K., Gustafson,A.M., Kasschau,K.D., Lellis,A.D., Zilberman,D., Jacobsen,S.E. and Carrington,J.C. (2004) Genetic and functional diversification of small RNA pathways in plants. *PLoS Biol.*, **2**, E104.
8. Donaire,L., Barajas,D., Martínez-García,B., Martínez-Priego,L., Pagán,I. and Llave,C. (2008) Structural and genetic requirements for the biogenesis of tobacco rattle virus-derived small interfering RNAs. *J. Virol.*, **82**, 5167–5177.
9. Qi,X., Bao,F.S. and Xie,Z. (2009) Small RNA deep sequencing reveals role for Arabidopsis thaliana RNA-dependent RNA polymerases in viral siRNA biogenesis. *PLoS ONE*, **4**, e4971.
10. Wang,X.B., Wu,Q., Ito,T., Cillo,F., Li,W.X., Chen,X., Yu,J.L. and Ding,S.W. (2010) RNAi-mediated viral immunity requires amplification of virus-derived siRNAs in Arabidopsis thaliana. *Proc. Natl Acad. Sci. USA*, **107**, 484–489.
11. Garcia-Ruiz,H., Takeda,A., Chapman,E.J., Sullivan,C.M., Fahlgren,N., Brempelis,K.J. and Carrington,J.C. (2010) Arabidopsis RNA-dependent RNA polymerases and Dicer-like proteins in antiviral defense and small interfering RNA biogenesis during Turnip Mosaic Virus infection. *Plant Cell*, **22**, 481–496.
12. Deleris,A., Gallego-Bartolome,J., Bao,J., Kasschau,K.D., Carrington,J.C. and Voinnet,O. (2006) Hierarchical action and inhibition of plant Dicer-like proteins in antiviral defense. *Science*, **313**, 68–71.
13. Bouché,N., Lauressergues,D., Gasciolli,V. and Vaucheret,H. (2006) An antagonistic function for Arabidopsis DCL2 in development and a new function for DCL4 in generating viral siRNAs. *EMBO J.*, **25**, 3347–3356.
14. Blevins,T., Rajeswaran,R., Shivaprasad,P.V., Beknazariants,D., Si-Ammour,A., Park,H.S., Vazquez,F., Robertson,D., Meins,F. Jr, Hohn,T. *et al.* (2006) Four plant Dicers mediate viral small RNA biogenesis and DNA virus induced silencing. *Nucleic Acids Res.*, **34**, 6233–6246.
15. Akbergenov,R., Si-Ammour,A., Blevins,T., Amin,I., Kutter,C., Vanderschuren,H., Zhang,P., Gruissem,W., Meins,F. Jr, Hohn,T. *et al.* (2006) Molecular characterization of geminivirus-derived small RNAs in different plant species. *Nucleic Acids Res.*, **34**, 462–471.
16. Moissiard,G. and Voinnet,O. (2006) RNA silencing of host transcripts by cauliflower mosaic virus requires coordinated action of the four Arabidopsis Dicer-like proteins. *Proc. Natl Acad. Sci. USA*, **103**, 19593–19598.
17. Guilley,H., Dudley,R.K., Jonard,G., Balàzs,E. and Richards,K.E. (1982) Transcription of Cauliflower mosaic virus DNA: detection of promoter sequences, and characterization of transcripts. *Cell*, **30**, 763–773.
18. Love,A.J., Laird,J., Holt,J., Hamilton,A.J., Sadanandom,A. and Milner,J.J. (2007) Cauliflower mosaic virus protein P6 is a suppressor of RNA silencing. *J. Gen. Virol.*, **88**, 3439–3444.
19. Haas,G., Azevedo,J., Moissiard,G., Geldreich,A., Himber,C., Bureau,M., Fukuhara,T., Keller,M. and Voinnet,O. (2008) Nuclear import of CaMV P6 is required for infection and suppression of the RNA silencing factor DRB4. *EMBO J.*, **27**, 2102–2112.
20. Shivaprasad,P.V., Rajeswaran,R., Blevins,T., Schoelz,J., Meins,F. Jr, Hohn,T. and Pooggin,M.M. (2008) The CaMV transactivator/viroplasmin interferes with RDR6-dependent trans-acting and secondary siRNA pathways in Arabidopsis. *Nucleic Acids Res.*, **36**, 5896–5909.
21. Pfeiffer,P. and Hohn,T. (1983) Involvement of reverse transcription in the replication of cauliflower mosaic virus: a detailed model and test of some aspects. *Cell*, **33**, 781–789.
22. Fütterer,J., Kiss-László,Z. and Hohn,T. (1993) Nonlinear ribosome migration on cauliflower mosaic virus 35S RNA. *Cell*, **73**, 789–802.
23. Hemmings-Mieszczak,M., Steger,G. and Hohn,T. (1997) Alternative structures of the cauliflower mosaic virus 35 S RNA leader: implications for viral expression and replication. *J. Mol. Biol.*, **267**, 1075–1088.

24. Guerra-Peraza,O., de Tapia,M., Hohn,T. and Hemmings-Mieszczak,M. (2000) Interaction of the cauliflower mosaic virus coat protein with the pregenomic RNA leader. *J. Virol.*, **74**, 2067–2072.
25. Pooggin,M.M., Fütterer,J. and Hohn,T. (2008) Cross-species functionality of pararetroviral elements driving ribosome shunting. *PLoS One*, **3**, e1650.
26. Kanno,T., Huettel,B., Mette,M.F., Aufsatz,W., Jaligot,E., Daxinger,L., Kreil,D.P., Matzke,M. and Matzke,A.J. (2005) Atypical RNA polymerase subunits required for RNA-directed DNA methylation. *Nat. Genet.*, **37**, 761–765.
27. Onodera,Y., Haag,J.R., Ream,T., Nunes,P.C., Pontes,O. and Pikaard,C.S. (2005) Plant nuclear RNA polymerase IV mediates siRNA and DNA methylation-dependent heterochromatin formation. *Cell*, **120**, 613–622.
28. Allen,E., Xie,Z., Gustafson,A.M. and Carrington,J.C. (2005) MicroRNA-directed phasing during trans-acting siRNA biogenesis in plants. *Cell*, **121**, 207–221.
29. Golden,T.A., Schauer,S.E., Lang,J.D., Pien,S., Mushegian,A.R., Grossniklaus,U., Meinke,D.W. and Ray,A. (2002) SHORT INTEGUMENTS1/SUSPENSOR1/CARPEL FACTORY, a Dicer homolog, is a maternal effect gene required for embryo development in Arabidopsis. *Plant Physiol.*, **130**, 808–822.
30. Jacobsen,S.E., Running,M.P. and Meyerowitz,E.M. (1999) Disruption of an RNA helicase/RNAse III gene in Arabidopsis causes unregulated cell division in floral meristems. *Development*, **126**, 5231–5243.
31. Shivaprasad,P.V., Akbergenov,R., Trinks,D., Rajeswaran,R., Veluthambi,K., Hohn,T. and Pooggin,M.M. (2005) Promoters, transcripts, and regulatory proteins of Mungbean yellow mosaic geminivirus. *J. Virol.*, **79**, 8149–8163.
32. Qi,Y. and Mi,S. (2010) Purification of Arabidopsis argonaute complexes and associated small RNAs. *Methods Mol. Biol.*, **592**, 243–254.
33. Turnage,M.A., Muangsan,N., Peele,C.G. and Robertson,D. (2002) Geminivirus-based vectors for gene silencing in Arabidopsis. *Plant J.*, **30**, 107–114.
34. Lu,C., Kulkarni,K., Souret,F.F., MuthuValliappan,R., Tej,S.S., Poethig,R.S., Henderson,I.R., Jacobsen,S.E., Wang,W., Green,P.J. *et al.* (2006) MicroRNAs and other small RNAs enriched in the Arabidopsis RNA-dependent RNA polymerase-2 mutant. *Genome Res.*, **16**, 1276–1288.
35. Kasschau,K.D., Fahlgren,N., Chapman,E.J., Sullivan,C.M., Cumbie,J.S., Givan,S.A. and Carrington,J.C. (2007) Genome-wide profiling and analysis of Arabidopsis siRNAs. *PLoS Biol.*, **5**, e57.
36. Kurihara,Y. and Watanabe,Y. (2004) Arabidopsis micro-RNA biogenesis through Dicer-like 1 protein functions. *Proc. Natl Acad. Sci. USA*, **101**, 12753–12758.
37. Vaucheret,H., Mallory,A.C. and Bartel,D.P. (2006) AGO1 homeostasis entails coexpression of MIR168 and AGO1 and preferential stabilization of miR168 by AGO1. *Mol. Cell*, **22**, 129–136.
38. Mi,S., Cai,T., Hu,Y., Chen,Y., Hodges,E., Ni,F., Wu,L., Li,S., Zhou,H., Long,C. *et al.* (2008) Sorting of small RNAs into Arabidopsis argonaute complexes is directed by the 5′ terminal nucleotide. *Cell*, **133**, 116–127.
39. Montgomery,T.A., Howell,M.D., Cuperus,J.T., Li,D., Hansen,J.E., Alexander,A.L., Chapman,E.J., Fahlgren,N., Allen,E. and Carrington,J.C. (2008) Specificity of ARGONAUTE7-miR390 interaction and dual functionality in TAS3 trans-acting siRNA formation. *Cell*, **133**, 128–141.
40. Takeda,A., Iwasaki,S., Watanabe,T., Utsumi,M. and Watanabe,Y. (2008) The mechanism selecting the guide strand from small RNA duplexes is different among argonaute proteins. *Plant Cell Physiol.*, **49**, 493–500.
41. Wierzbicki,A.T., Haag,J.R. and Pikaard,C.S. (2008) Noncoding transcription by RNA polymerase Pol IVb/Pol V mediates transcriptional silencing of overlapping and adjacent genes. *Cell*, **135**, 635–648.
42. Al-Kaff,N.S., Covey,S.N., Kreike,M.M., Page,A.M., Pinder,R. and Dale,P.J. (1998) Transcriptional and posttranscriptional plant gene silencing in response to a pathogen. *Science*, **279**, 2113–2115.
43. Gómez,G., Martínez,G. and Pallás,V. (2009) Interplay between viroid-induced pathogenesis and RNA silencing pathways. *Trends Plant Sci.*, **14**, 264–269.
44. Lipardi,C. and Paterson,B.M. (2009) Identification of an RNA-dependent RNA polymerase in Drosophila involved in RNAi and transposon suppression. *Proc. Natl Acad. Sci. USA*, **106**, 15645–15650.
45. Pooggin,M.M., Fütterer,J., Skryabin,K.G. and Hohn,T. (1999) A short open reading frame terminating in front of a stable hairpin is the conserved feature in pregenomic RNA leaders of plant pararetroviruses. *J. Gen. Virol.*, **80**, 2217–2228.
46. Pooggin,M.M., Hohn,T. and Fütterer,J. (1998) Forced evolution reveals the importance of short open reading frame A and secondary structure in the cauliflower mosaic virus 35S RNA leader. *J. Virol.*, **72**, 4157–4169.
47. Pooggin,M.M., Fütterer,J., Skryabin,K.G. and Hohn,T. (2001) Ribosome shunt is essential for infectivity of cauliflower mosaic virus. *Proc. Natl Acad. Sci. USA*, **98**, 886–891.
48. Bortolamiol,D., Pazhouhandeh,M., Marrocco,K., Genschik,P. and Ziegler-Graff,V. (2007) The Polerovirus F box protein P0 targets ARGONAUTE1 to suppress RNA silencing. *Curr. Biol.*, **17**, 1615–1621.
49. Baumberger,N., Tsai,C.H., Lie,M., Havecker,E. and Baulcombe,D.C. (2007) The Polerovirus silencing suppressor P0 targets ARGONAUTE proteins for degradation. *Curr. Biol.*, **17**, 1609–1614.
50. Azevedo,J., Garcia,D., Pontier,D., Ohnesorge,S., Yu,A., Garcia,S., Braun,L., Bergdoll,M., Hakimi,M.A., Lagrange,T. *et al.* (2010) Argonaute quenching and global changes in Dicer homeostasis caused by a pathogen-encoded GW repeat protein. *Genes Dev.*, **24**, 904–915.
51. Várallyay,E., Válóczi,A., Agyi,A., Burgyán,J. and Havelda,Z. (2010) Plant virus-mediated induction of miR168 is associated with repression of ARGONAUTE1 accumulation. *EMBO J.*, **29**, 3507–3519.
52. Itaya,A., Zhong,X., Bundschuh,R., Qi,Y., Wang,Y., Takeda,R., Harris,A.R., Molina,C., Nelson,R.S. and Ding,B. (2007) A structured viroid RNA is substrate for Dicer-like cleavage to produce biologically active small RNAs but is resistant to RISC-mediated degradation. *J. Virol.*, **81**, 2980–2994.
53. Gómez,G. and Pallás,V. (2007) Mature monomeric forms of Hop stunt viroid resist RNA silencing in transgenic plants. *Plant J.*, **51**, 1041–1049.
54. Wang,M.B., Bian,X.Y., Wu,L.M., Liu,L.X., Smith,N.A., Isenegger,D., Wu,R.M., Masuta,C., Vance,V.B., Watson,J.M. *et al.* (2004) On the role of RNA silencing in the pathogenicity and evolution of viroids and viral satellites. *Proc. Natl Acad. Sci. USA*, **101**, 3275–3280.
55. Szittya,G., Molnár,A., Silhavy,D., Hornyik,C. and Burgyán,J. (2002) Short defective interfering RNAs of tombusviruses are not targeted but trigger post-transcriptional gene silencing against their helper virus. *Plant Cell*, **14**, 359–372.
56. Andersson,M.G., Haasnoot,P.C., Xu,N., Berenjian,S., Berkhout,B. and Akusjärvi,G. (2005) Suppression of RNA interference by adenovirus virus-associated RNA. *J. Virol.*, **79**, 9556–9565.